

Impacts of a changing environment on a stoichiometric producer-grazer system: a stochastic modelling approach

Velizar Kirkow^{a,b,*}, Hao Wang^a, Pablo Venegas Garcia^a, Shohel Ahmed^a, Christopher M. Hegrud^a

^a Department of Mathematical and Statistical Sciences, University of Alberta, Edmonton, AB T6G 2G1, Canada

^b Department of Mathematics, CEMPS, University of Exeter

ARTICLE INFO

Keywords:

Predator-prey system
Stochastic modelling
System of differential equations
Climate Change

ABSTRACT

Internal and external factors on a producer-grazer system are important because these systems underpin many food chains and changes in them are therefore significant for many animal species. In particular, alterations between *phytoplankton* and *zooplankton* are important because they represent a vast source of nutrients for aquatic species. However, the impacts of different intrinsic and extrinsic noise on *phytoplankton* and *zooplankton* population dynamics are still missing. By applying stochastic methods to a popular stoichiometric model, the influence of internal and external factors on the system are explored, culminating with a proposition of how noise in the system can be used to examine the latitudinal spatial distribution of *phytoplankton*. This is achieved by expanding the stoichiometric model to account for macro environmental factors that induce noise in the system. First, the population dynamics under the influence of factors, such as predation, wind gusts and temperature, are individually documented in the paper. Thereafter, using the macro environmental factors such as climate change, stochastic simulations generate a spatial distribution in a latitudinal sense of *phytoplankton* where it is observed that the *phytoplankton* clusters are blooming at a higher than expected latitude. Therefore, the latitudinal distribution of *phytoplankton* of these clusters gives further evidence of the influence of arctic amplification.

1. Introduction

Ecological stoichiometry is the study of the balance of energy (such as light and carbon) and elemental resources (such as phosphorus and nitrogen) by applying the law of conservation of mass to ecological interactions and processes (Sturner and Elser, 2017). The scarcity of any of such elements can strongly restrict cellular and organismal growth since herbivorous grazers are assumed to have higher nutrient requirements than the producer they consume. The growth of grazers can be limited either by the quantity or quality of plants (Urabe et al., 2002). The classical mathematical models, such as Lotka-Volterra type predator-prey models (Edelstein-Keshet, 2005), that consider energy flow in the form of population or density cannot explain many observed ecological phenomena. For example, for very high light intensity, the nonstoichiometric Lotka-Volterra model cannot explain a case where high phytoplankton abundance does not result in high grazer abundance (Elser and Kuang, 2002). This is because the high phytoplankton abundance allows them to become phosphorus limited under the

increased photosynthetic rate, and therefore they can limit grazer growth due to being poor quality food relative to the requirement of the grazer. One of the well-received stoichiometric producer-grazer models to deal with this counterexample is known as the LKE model (attributed to Loladze, Kuang and Elser) that was formulated in Loladze et al. (Loladze et al., 2000). Considering the idea of energy dissipation through different trophic levels, the LKE model was developed to consider the energy flow, through chemical energy, in predator-prey systems like the classical Lotka-Volterra equations (Loladze et al., 2000). In this paper, we consider the 'prey' as a primary producer, such as *phytoplankton*, and the 'predator' as a grazer, such as *zooplankton*. This model tracks only two elements, carbon (C) and phosphorus (P), where all others are assumed to be sufficiently abundant. Despite the non-linearity of the LKE model, some rigorous mathematical analysis has been completed in (Loladze et al., 2000, Li et al., 2011, Xie et al., 2018), by considering different consumption rates of grazer (per day), which is usually one of the Holling-type functional responses. Though a biological system can be impacted by chemical imbalance, this paper

This work was supported by the MITACS Globalink Internship, University of Alberta and University of Exeter

* Corresponding author: Mr Velizar Kirkow, University of Exeter College of Engineering Mathematics and Physical Sciences, United Kingdom

<https://doi.org/10.1016/j.ecolmodel.2022.109971>

Received 21 October 2021; Received in revised form 27 March 2022; Accepted 31 March 2022

0304-3800/© 2022 The Author(s). Published by Elsevier B.V. This is an open access article under the CC BY license (<http://creativecommons.org/licenses/by/4.0/>).

explores the dynamics of the system due to the noise induced within the system.

Biological systems are inevitably affected by various noises which can be important or even dominant in controlling dynamics of trophic interactions (Yuan et al., 2020). Over the past several decades, the qualitative behaviour of the deterministic model has been extensively studied under the influence of noise (Xu et al., 2016, Vadim Anishchenko and Astakhov, 2007, Horsthemke, 1984, Gao et al., 1999, Kim et al., 1998, Kraut and Feudel, 2002). In (Xu et al., 2016), the coexistence states are perturbed to extinction for a noise induced chemostat model. Also, the presence of coexisting attractors under noise can generate new dynamic regimes (Vadim Anishchenko and Astakhov, 2007). The presence of noise in nonlinear dynamical models show various new phenomena not observed in the deterministic case, such as noise-induced transitions (Horsthemke, 1984), noise induced chaos (Gao et al., 1999), and noise-induced multistability (Kim et al., 1998, Kraut and Feudel, 2002). We know that many biological and environmental parameters (for example, light intensity, tidal circulation, nutrient availability, water temperature, eutrophication, acidity, etc.) are inevitably subject to fluctuation in time. Hence, the environmental random disturbances can change the dynamical behaviours of the competitive models in chemostats (Xu and Yuan, 2016, Zhao and Liu, 2019, Xingwang Yu, 2020) and the producer-grazer models (Yu Zhao and Yuan, 2015, Xingwang Yu and Yuan, 2018, Yu et al., 2019, Yu et al., 2019, Yuan et al., 2020, Wang and Liu, 2020). Incorporating stochasticity under climatology in population dynamics became popular day by day due to the large sensitivity of climate models to small perturbations (Palmer and Williams, 2008). The aim of this paper is to study the phenomena of noise-induced transitions for the LKE model with a nonlinear Holling-type II consumption rate for the grazer.

In view of the aforementioned in Section 2 we propose a new deterministic stoichiometric producer– grazer model which is the extension of the LKE model by inclusion of a new equation for the change in light-dependent carrying capacity, and then we propose its stochastic version by taking into account environmental variation. In order to reveal the internal and external effects of environmental fluctuations on the dynamics for explaining the nature of the steady state, we investigate the time to first transition in Section 3. Section 4 investigates temperature and latitude dependent induced noise where the spatial distribution of *phytoplankton* and *zooplankton* clusters is discussed. Finally, the influence of arctic amplification in *phytoplankton* clusters are discussed in Section 5 to conclude the paper.

2. Model

The LKE model framework is based on ecological stoichiometric constraints which have been adapted by the Liebig’s Law of Minimum (Loladze et al., 2000). The producer exhibits logistic growth limited either by energy or by the availability of phosphorus in the absence of the grazer. On the other hand, the growth of the grazer is limited either by the amount of producer carbon available or phosphorus available relative to their needs. The LKE model was used to deal with this situation, and one of its formulations is stated as follows:

$$\begin{aligned} \frac{dx}{dt} &= bx \left(1 - \frac{x}{\min\left\{K, \frac{P - \theta y}{q}\right\}} \right) - \frac{cxy}{a + x} - \delta x \\ \frac{dy}{dt} &= e \min\left\{1, \frac{(P - \theta y)/x}{\theta}\right\} \frac{cxy}{a + x} - dy \end{aligned} \tag{1}$$

where x and y represent the biomasses of *phytoplankton* (producer) and *zooplankton* (grazer) over time in carbon units, respectively. In modelling the consumption rate of the grazer, we chose Holling type II as the functional response as it gives a more realistic representation of the system by considering predator satiation, where the gradient of the

functional response decreases monotonically (Dawes and Souza, 2013). Moreover, model (1) has already been extensively studied in the literature (Li et al., 2011, Xie et al., 2018). All the variable descriptions for the LKE model with their corresponding numerical values are provided in Table 1. In eq. (1), we have included a general predation term, δx , for grazing from higher trophic levels. However, literature suggests that this term is small and we have assumed it to be negligible (Costa et al., 2009)

Under climate change, increased light intensity as well as temperature increase, would lead to an overall increase in light-dependent carrying capacity (K) explicitly. Therefore, variation in light directly affects the growth of *phytoplankton* and as a consequence that of *zooplankton* in an indirect manner due to the system coupling (Metsoviti et al., 2020)]. The underlying mathematics for the construction of the differential equation describing K is inspired by the climate change model (Bellouin et al., 2020):

$$\dot{Q}' \approx \lambda T'_s \tag{2}$$

Equation (2) gives a simple definition of how a forcing in the system (Q' [Wm^{-2}]) (change in the energy balance) leads to the climate system experiencing a temperature change ($T'_s[K]$) due to the system feedback ($\lambda[Wm^{-2}K^{-1}]$, where the negative sign comes from the orientation of negative feedback. In practice, Eq. (2) is a saturating function representing how the earth’s temperature changes with respect to a change in forcing. Carrying capacity is a multi-faceted part of a biological system that is linked to many different variables to influence its value over time. We assume that under climate change, $K(t)$ varies from an initial value to a final value, and that the boundedness condition of $K(t)$ is satisfied even under environmental change. We consider this because carrying capacity is a flexible term in ecology that can be adapted and broadly interpreted (Chapman and Byron, 2018). Periodic fluctuations are neglected because $K(t)$ is not directly light intensity. The general equation for $K(t)$ is given by the following equation:

$$K(t) = K_L + (K_U - K_L) \tanh(t), \tag{3}$$

where K_L is the initial value and K_U is the final value of $K(t)$, respectively. Graphically the behaviour of $K(t)$ is shown in Fig. 1 with $K_L = 0.567$, $K_U = 1$ and for this range of K , the system is light-limited as $\min\{K, (P - \theta y)/q\} = K$ therefore inorganic environmental factors are the focus of the paper. In order to account for $K(t)$ increasing from an initial value to a final one, the equation for light-dependent carrying capacity involves a saturating function which varies in the range between 0 and 1, where the choice of a hyperbolic tangent function is inspired by the Morris-Lecar model (Lecar, 2007). By design, the function only requires lower and upper numerical value inputs for light-dependent carrying capacity which makes the extended version of the LKE model as follows:

Table 1
Numerical values of the parameters with definitions taken from (Yuan et al., 2020)

Parameter	Definition	Numerical value	Unit
K	Light-dependent carrying capacity	[0,2]	mgC/L
P	Total phosphorus	0.0246	mgP
q	Minimum P:C ratio (<i>phytoplankton</i>)	0.004	mgP/ mgC
θ	Constant P:C ratio (<i>zooplankton</i>)	0.04	mgP/ mgC
b	Maximum growth rate (<i>phytoplankton</i>)	1.2	/day
e	Conversion efficiency (<i>zooplankton</i> from <i>phytoplankton</i>)	0.8	/day
d	Mortality rate (<i>zooplankton</i>)	0.25	/day
c	Maximal predation rate	0.8	/day
a	Half-saturation constant for predation	0.25	mgC/L
p	p/θ	0.615	mgC

Table 2
Bounds of light intensity.

Term in Eq. (10)	Meaning
$E(\varphi)$	Incident radiation at latitude (Wm^{-2})
φ	Latitude (degrees from the equator), $\varphi \in [-90, 90]$
S	Solar constant (Wm^{-2})
a	Albedo $a \in [0, 1]$

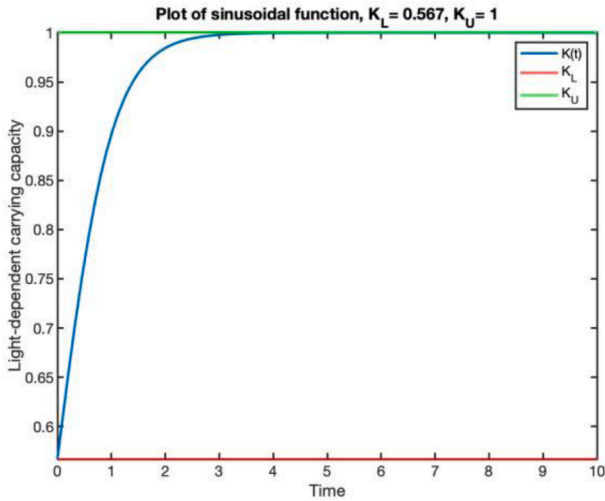


Fig. 1. Saturating function $K(t)$.

$$\begin{aligned} \frac{dx}{dt} &= bx \left(1 - \frac{x}{\min\left\{K, \frac{P - \theta y}{q}\right\}} \right) - \frac{cxy}{a+x} \\ \frac{dy}{dt} &= emin \left(1, \frac{(P - \theta y)/x}{\theta} \right) \frac{cxy}{a+x} - dy \\ \frac{dK}{dt} &= (K_U - K_L) \text{sech}^2(t) \end{aligned} \tag{4}$$

Noise (either additive or multiplicative) is fundamental to biological systems because it is able to account for the unpredictability of intracellular reactions and extracellular interactions. Stochastic differential equations (SDEs) are more suitable for modelling biological systems than mechanistic models since SDEs add the inherent unpredictability of internal cellular activities to biological systems. In this paper, noise is made such that it is multiplicative which takes into account the state of the system and is, therefore, more useful for non-linear systems (Gottwald and Harlim, 2013). Multiplicative noise also helps the system satisfy the biological constraints that the populations must be greater than or equal to 0 where $x \geq 0$ and $y \geq 0$. In this paper we use the common definition of noise as the ratio between the standard deviation of the variable and the mean:

$$\varepsilon_i = \frac{\sigma_i}{\mu_i}, \text{ coefficient of variation} \tag{5}$$

The stochastic version of the deterministic system (4) is given by the following system by adding Wiener processes for the noise terms:

$$\begin{aligned} dx &= \left[bx \left(1 - \frac{x}{\min\left\{K, \frac{P - \theta y}{q}\right\}} \right) - \frac{cxy}{a+x} \right] dt + \varepsilon_x x dB_1 \\ dy &= \left[emin \left\{ 1, \frac{(P - \theta y)/x}{\theta} \right\} \frac{cxy}{a+x} - dy \right] dt + \varepsilon_y y dB_2 \\ dK &= [(K_U - K_L) \text{sech}^2 t] dt + \varepsilon_K K dB_3 \end{aligned} \tag{6}$$

Here, ε_x , ε_y and ε_k represent intrinsic (in subsection 3.1) and/or extrinsic noises (in subsection 3.2). The complete expression of these noise terms is given by Eq. (13). The merits of using a stochastic model (6) over a mechanistic one (4) can be demonstrated by Figs 2 and 3 with initial conditions $[x(0), y(0), K(0)] = [0.1603, 0.4415, 0.567]$ and $[\varepsilon_k, \varepsilon_y, \varepsilon_k] = [0.0015, 0, 0.0015, 0]$ (here we consider intrinsic noise). Fig. 2a shows the population dynamics are regular in a limit cycle and Fig. 2b shows they are smooth and the varying K does not play any role. The stochasticity in Figs 3a and 3b demonstrate the irregularity of biological systems (Sabino et al., 2018). Therefore, for the rest of the paper, a stochastic interpretation of LKE model will be made to account for the irregularity of intracellular and extracellular interactions as well as their unpredictability. It is intuitive that in the presence of noise, a solution of a bistable system may switch from one attractor to the other.

Determining how long this takes to happen on average is called mean time to first passage or time to first transition (see details in Sections 3 and 4).

The differential equation for $K(t)$ has a deterministic definition (as shown by Eq. (3) and in the system (4)). In order to utilize (6) to investigate noise more explicitly, we propagate noise through the influence of latitudinal distribution. We approach this by using the principle of the simple energy balance equation for change in temperature equilibrium and the absorption of radiation by the atmosphere. One of the main ways in which they are related is due to latitude because the angle of incidence at the equator is shallower than at higher latitudes. The discussion of latitude-dependence for light-dependent carrying capacity will begin with the equation for zonal temperature (Marshall and Plumb, 1989):

$$T(\varphi) = \left(\frac{(1-a)S\cos(\varphi)}{\pi\varepsilon\sigma} \right)^{\frac{1}{4}}. \tag{7}$$

By using the Stefan-Boltzmann law for radiation, terms such as emissivity (ε) are dropped (Marshall and Plumb, 1989) and $E(\varphi)$ represents energy flux per unit area:

$$E = \varepsilon\sigma T^4. \tag{8}$$

By rearranging Eq. (7), we obtain

$$\varepsilon\sigma T^4 = \frac{(1-a)S\cos(\varphi)}{\pi}. \tag{9}$$

Hence the latitude-dependent equation for radiation is

$$E(\varphi) = \frac{(1-a)S\cos(\varphi)}{\pi}. \tag{10}$$

Equation (10) is a highly simplified expression of the energy flux on earth from solar energy since only energy balance arguments have been applied. For simplicity, we solely focus on noise that encompasses the scope of the atmospheric interactions instead of deterministic expressions of light intensity. The reasoning behind this is that atmospheric light scattering increases with latitude due to the angle of incidence where light photons must pass through more atmosphere to reach the earth's surface. Herewith yielding a proposition for a simple formula for noise in the changing environment (see more in Section 4) which is now used to define noise on $K(t)$:

$$\varepsilon_K = \varepsilon_3(1 + |\sin(\phi)|). \tag{11}$$

According to the global phytoplankton audit, phytoplankton are mostly distributed in equatorial and mid-latitude regions (see Fig. 14) which means that one does not need to take into account arctic regions where there are months of continued sunlight for which additional care needs to be taken when modelling for light.

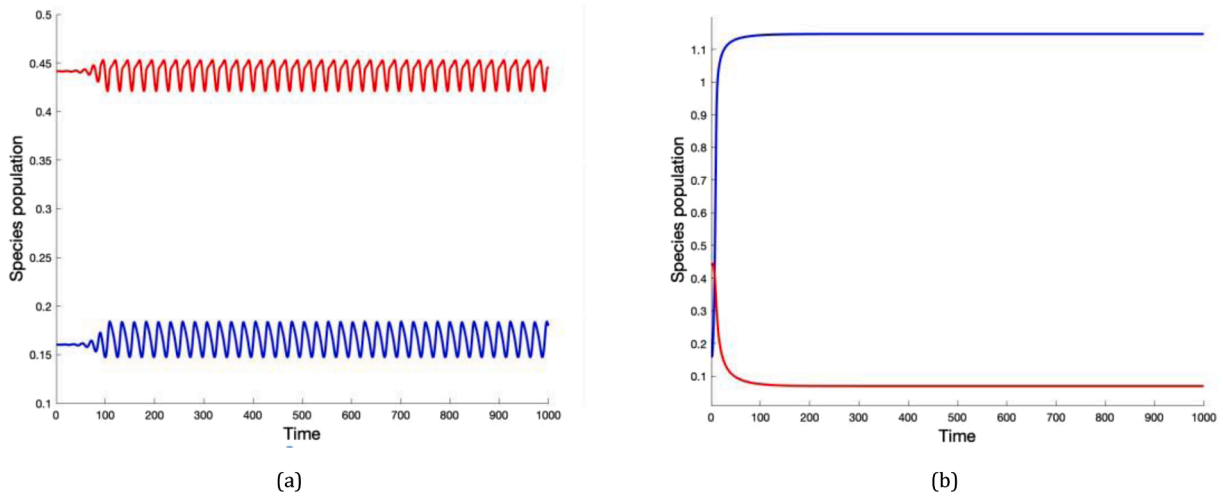


Fig. 2. Time simulations for the Mechanistic LKE model - Eq. (4) with *phytoplankton* abundance shown in red, and *zooplankton* abundance in blue. In (a) we take constant K ($K_L = K_U = 0.567$); in (b) we vary K ($K_L = 0.567$, $K_U = 1$).

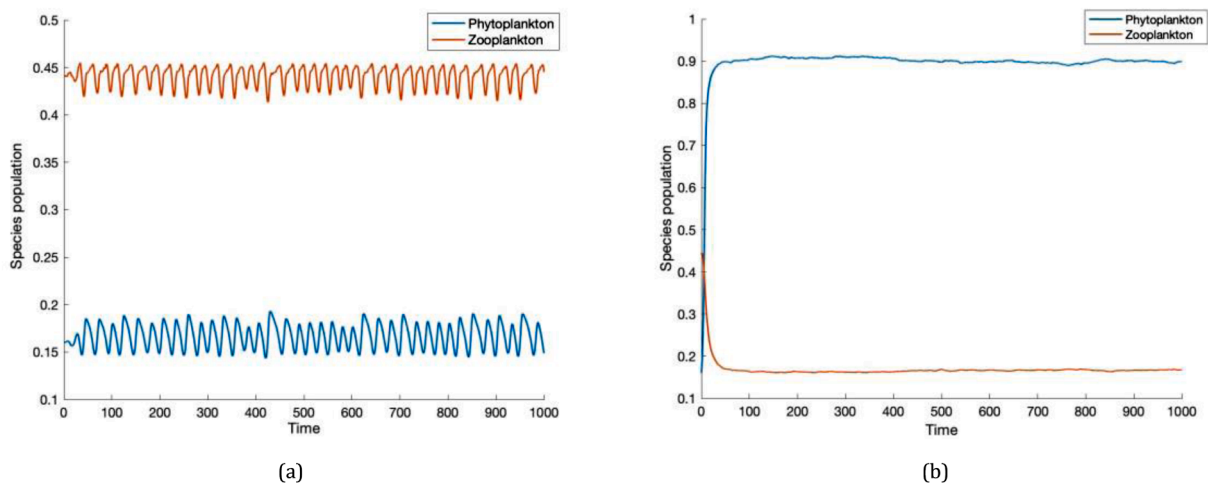


Fig. 3. (a): K stays constant but noise causes similar change as in Fig. 2a. (b): K changes from $K_L = 0.567$ to $K_U = 1$; similar change as in Fig. 2b.

3. Methods

Noise is an integral part of any biological system and a natural by-product of the complexity and scope of interactions that occur in a biosphere. Here we introduce noise via an intrinsic and extrinsic context to model Eq. (6). Intrinsic noise in a biological system is defined as the stochasticity of biochemical interactions of particles (Lei et al., 2015). In a more practical sense, intrinsic noise gives a margin of error when taking into the account the sheer number of biochemical reactions taking place within the organisms. So far intrinsic noise has been dominant in Figs 3a and 3b and we discuss it in terms of the time to first transition. There also exists extrinsic noise that is due to environmental fluctuations. Examples of extrinsic noise include temperature, fluctuations in carrying capacity, and sudden events (such as predation). Extrinsic noise is defined as in Eq. (5). Noise in a mathematical sense can be either additive or multiplicative. In this paper, noise is made such that it is multiplicative. Multiplicative noise takes into account the state of the system and is therefore more useful for non-linear systems (Gottwald and Harlim, 2013). However the main justification for multiplicative noise is that that it helps the system uphold the biological constraints of $x > 0, y > 0$ even when the system is stochastic and is volatile by construction.

3.1. Intrinsic noise

We will begin by considering intrinsic noise explicitly for the stochastic model (6). Although intrinsic noise is being considered (denoted by $\varepsilon_i \in [1, 3]$), let $\varepsilon_x = \varepsilon_1$, $\varepsilon_y = \varepsilon_2$ and $\varepsilon_K = \varepsilon_3$ such that there is no confusion about how noise was used for model (6). We denote \bar{x} as the average (time to first transition) TFT based on 5000 stochastic simulations as the time in which a transition from E_2 to E_4 . As the intrinsic noise in the system was varied, the results for which are shown in table 3.

It is unsurprising that with a greater amount of noise, the time to first transition has a negative trend (see Fig. 5). The superposition of a linear regression model on the average time to first transition is shown in Fig. 5 as well where the normal linear model which is fitted to this data is described by

$$-19.584(\varepsilon_1 \times 10^3) + 855.2392 \quad (12)$$

The SRCC (spearman's rank correlation coefficient) for model (12) is -0.9761905 and therefore is a near perfect fit to our simulated data. This means that it is not beyond reason to investigate the model's predictive ability for time to first transition. From Table 4, it is clear that for small extrapolations, the normal linear model (NLM) has a strong predictive ability but as the extrapolation gets bigger, the predictive ability decreases significantly.

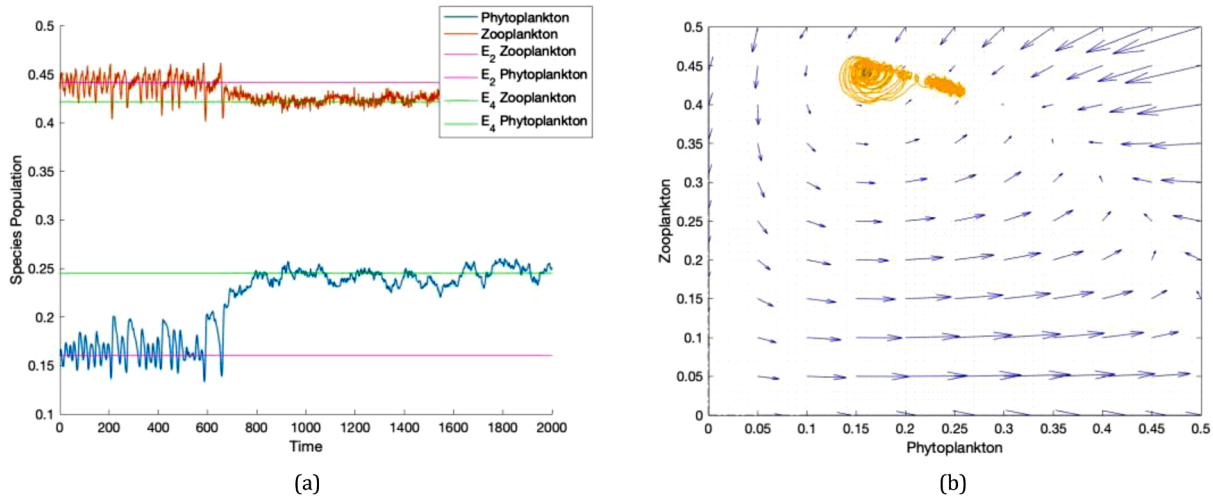


Fig. 4. (a): Example noise-induced oscillations for the case of $\epsilon_x = 0.001, \epsilon_x = 0.008, \epsilon_K = 0$, values of which are taken from (Yuan et al., 2020). (b): Phase plane for example oscillation for the case of $\epsilon_x = 0.001, \epsilon_x = 0.008, \epsilon_K = 0$, where transition to E_4 attracting basin is shown from E_2 .

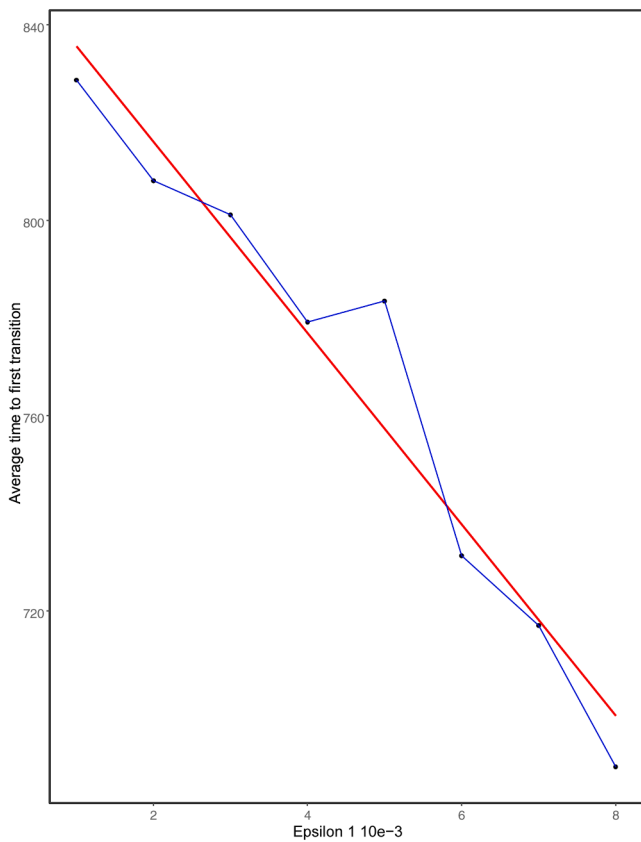


Fig. 5. Time of first return when varying ϵ_1 . Blue curve: line graph of the points, Red curve: fitted normal linear model.

Table 4
Predicted and simulation times for time to first transition.

ϵ_1	ϵ_2	Predicted	Simulation	Percentage error
0.012	0.008	620.2216	564.8108	9.8%
0.009	0.008	678.976	661.7874	0.026%

3.2. Extrinsic noise

Here we introduce the effects of predation on *zooplankton* via consideration of extrinsic noise attributable to interaction with their environment. A more complete understanding of the biological system happens with consideration of external predation on the coupled system (1) since in the natural environment, the coupled system is not isolated. *Zooplankton* have many predators but of particular interest is predation due to small fish. *Zooplankton* temporarily increase fecundity as a compensating feature when in the presence of predatory fish. Maternal *zooplankton* do this when exposed to kairomones and AgNPs and fecundity increases by a factor of up to 2. This phenomena is captured in our model by replacing $\frac{c\epsilon y}{a+x}$ with $\frac{c\epsilon y}{a+x} \times 2$ for a short amount of time (Hartmann et al., 2020).

Predation on *zooplankton* can be considered a ‘sudden’ event due to the differences between the time scale of population dynamics and predation duration. Fig. 6a shows how prior to the sudden event oscillations are present (limit cycle around E_2) and stabilise near E_4 afterwards (see Figs 6a and 6b). The sudden event scenario is modelled by a poisson-distributed random variable (where T_{max} is the maximum amount of time the system is considered for), where the rate parameter is set as

$$\lambda = \frac{T_{max}}{\text{Feeding frequency}}$$

Now, we introduce the effects of a weather-influenced sudden event that causes a population decrease in both *phytoplankton* and *zooplankton*. We assume the emergence of a sudden strong gust of wind as being the sudden event in question. Unlike the sudden event of predation, neither *phytoplankton* nor *zooplankton* have the opportunity to compensate for this. Furthermore, a sudden strong gust of wind would affect both *phytoplankton* and *zooplankton*. Further still, as a consequence of the strong sudden gust of wind, the carrying capacity of the system will also be decreased. As before, the strong wind will happen as a poisson process with a rate parameter similar to predation:

$$\lambda = \frac{T_{max}}{\text{Gust frequency}}$$

where T_{max} is the maximum amount of time over which the system is considered over. *phytoplankton* and *zooplankton* are not exclusively water surface-dwelling organisms, they can be observed at some depth. Using the ideas from (Blottiere, 2015), the model will assume that the water body is a lake. With the occurrence of a sudden gust of wind, a

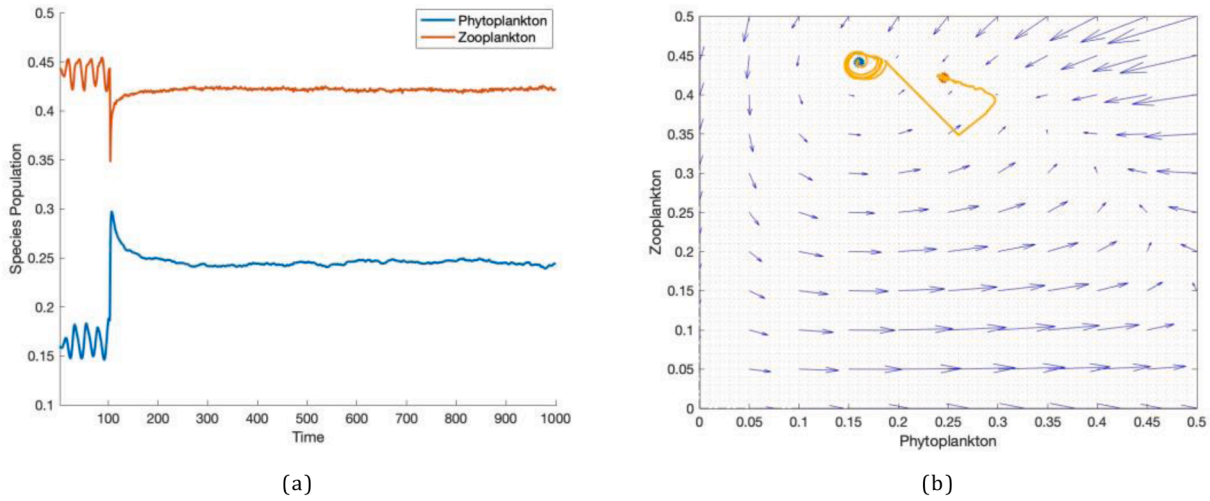


Fig. 6. (a): Populations of species with sudden events; predation is set up as a poisson distributed random variable, population of *zooplankton* halves and the fecundity doubles. (b): Phase plane of species with sudden events; predation is set up as a poisson distributed random variable, population of *zooplankton* halves and the fecundity doubles.

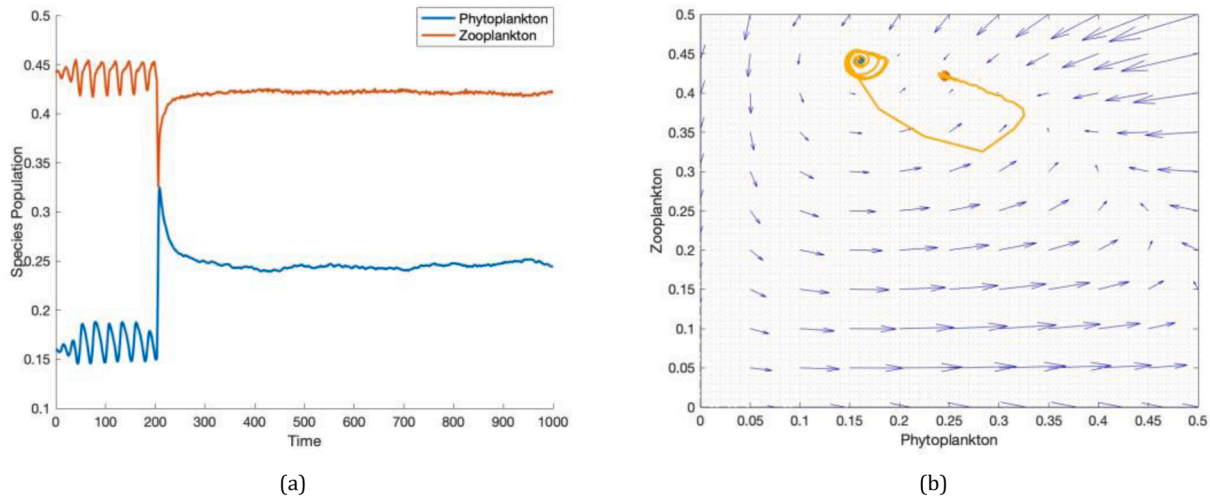


Fig. 7. (a): Populations of the two species with sudden events; Predation is set up as a Poisson process and the population of *zooplankton* decreases by a factor of 0.2 a day and the fecundity increases by a factor of 1.14 each day such that the net decrease in *zooplankton* is spread out over a time interval. (b): Phase plane with same set-up.

wave will be induced with height of

$$h = 0.105\sqrt{\text{fetch}}$$

where ‘fetch’ is the distance (m) over the surface of the lake that the wind blows over. The idea is that the propagation of a wave along the water surface would create turbulence where *phytoplankton* and *zooplankton* are; displacing a proportion of both organisms from their original position. Another assumption in this model is that the lake is no deeper than 100m, this is because the maximum depth at which *phytoplankton* have been observed to exist is 100m. The proportion of *phytoplankton* that are ‘swept’ away will be the ratio of h : *depth*. Assuming also that *zooplankton* are equally distributed with *phytoplankton* in the water column, the same ratio of *zooplankton* will be swept away as *phytoplankton*. In this light, it is intuitive to assume that the light-dependent carrying capacity will also be reduced by the same proportion. With this particular fetch and depth, the ratio (h :*depth*) \approx 33: 1000.

Figs 8a and 8b show that a sudden reduction in light-dependent carrying capacity leads to a destabilisation within the system and widening of oscillations around E_2 on a limit cycle.

The following Sections will consider light-dependent carrying capacity changing gradually as an investigation into the impact of climate change.

Here we introduce the effects of temperature on the populations of *phytoplankton* and *zooplankton* which is the second of the macro environmental factors considered, the first of which is implemented into the model. The larger the fluctuation, the larger the noise induced into the system due the environmental conditions changing from their optimal as per the definition of (5). In the particular case of the LKE model, temperature fluctuations do not induce noise uniformly into both species. This is because *phytoplankton* has an optimal temperature range of $T_{\text{phytoplankton}} \in [20, 30]^{\circ}\text{C}$ (Yu et al., 2019, Gottwald and Harlim, 2013) $^{\circ}\text{C}$ (Singh and Singh, 2015) whereas *zooplankton* has a smaller optimal temperature range: $T_{\text{zooplankton}} \in \{25\}^{\circ}\text{C}$ (Khan and Khan, 2008). The additional noise induced into *zooplankton* which is added to y is given by

$$\alpha_2 = \frac{\bar{T} - 25}{\bar{T}}$$

On the other hand additional noise induced into *phytoplankton* is given

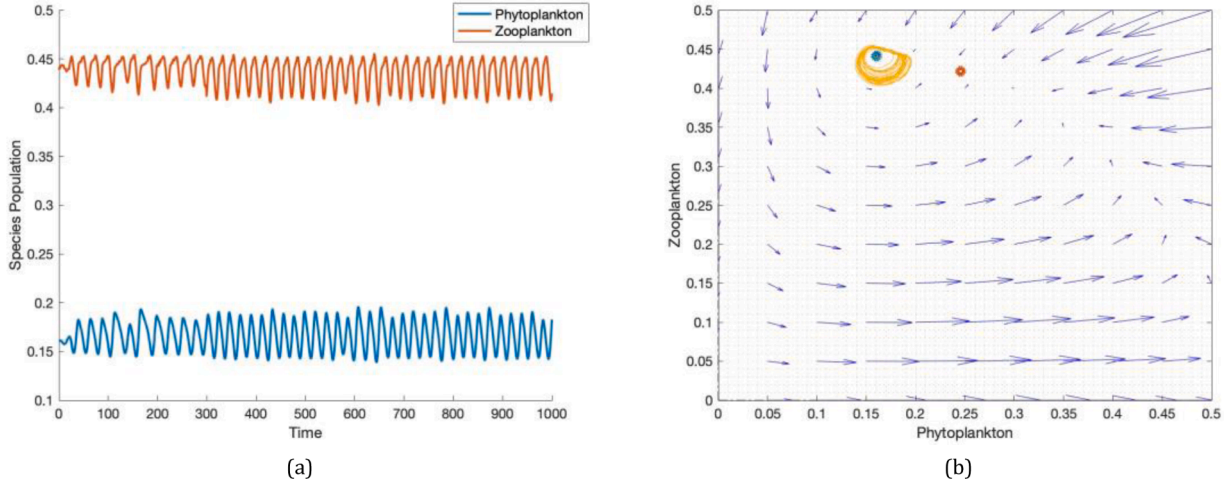


Fig. 8. (a): Population dynamics in shallow lake under the influence of sudden strong gust of wind with fetch:= 1km, depth:= 100m. (b): Phase plane with same set-up.

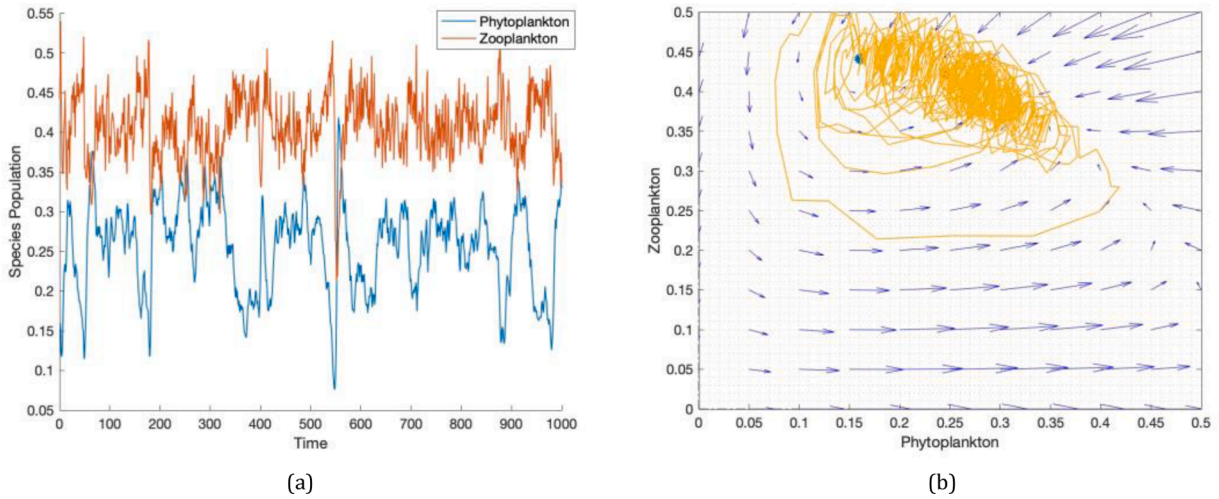


Fig. 9. (a): Populations of species with temperature noise; $\bar{T} = 20$, $K = 0.567$ and does not vary. (b): Phase plane of species with temperature noise; $\bar{T} = 20$, $K = 0.567$ and does not vary.

by:

$$\alpha_1 \begin{cases} \frac{|\bar{T} - 20|}{\bar{T}} & \text{for } \bar{T} < 20^{\circ}C \\ 0 & \text{for } 20^{\circ}C \leq \bar{T} \leq 30^{\circ}C \\ \frac{|\bar{T} - 30|}{\bar{T}} & \text{for } \bar{T} > 30^{\circ}C \end{cases}$$

where $\{\epsilon_1, \epsilon_2\}$. is intrinsic noise in the system due to inter-cellular biochemical reactions and $\{\alpha_1, \alpha_2\}$ is the extrinsic noise attributable to temperature. The temperature-induced noise is defined as

$$\epsilon_x = \epsilon_1 + \alpha_1, \epsilon_y = \epsilon_2 + \alpha_2$$

The last macro environmental factor and type of extrinsic noise is due to latitude dependence. The value for $\epsilon_3(0.005)$ was calculated with information about the absorption coefficient of the atmosphere from (Wei et al., 2018) per unit area; 0.001444 at the top of the Tropopause and 0.009025 at the Earth's surface. Then to make this part of the wiener process accounting for scintillation, we took the average of these two values.

To ascertain an idea for what the effects for zonally-dependent noise and varying light-dependent carrying capacity ($K_L = 0.567$ and $K_U =$

0.7), two latitudes were simulated. The noise in the system is such that the system, being bistable oscillates between equilibria. The results of Figs 11a and 11b predictably have less aggressive oscillations due to latitude-induced noise (in Eq. (11)) being smaller at lower latitudes.

From Fig. 12a, it is clear that with the background impact of the saturating function from Eq. (3), the system experiences an initial period of time with a highly dominant phytoplankton population due to the increase in light-dependent carrying capacity. In Fig. 12b, we have

$$E_2 = (0.1603, 0.4415) \text{ (Blue dot)}, E_4 = (0.2454, 0.4215) \text{ (Red dot)}.$$

Therefore even if K varies, the system has a tendency to return to oscillating between the original two steady states over a long enough period of time.

4. Results

Temperature and latitudinal noises are sources of extrinsic noises for the system. We apply them to the stochastic model (6) and measure their influence on the system using time to first transition. $K(t)$ is simulated with latitude-dependent noise and in order to simulate the time taken to first transition, the upper bound of $K(t)$ is omitted as discovered in the discussion surrounding Fig. 12a. Instead, variation in $K(t)$ is given as a

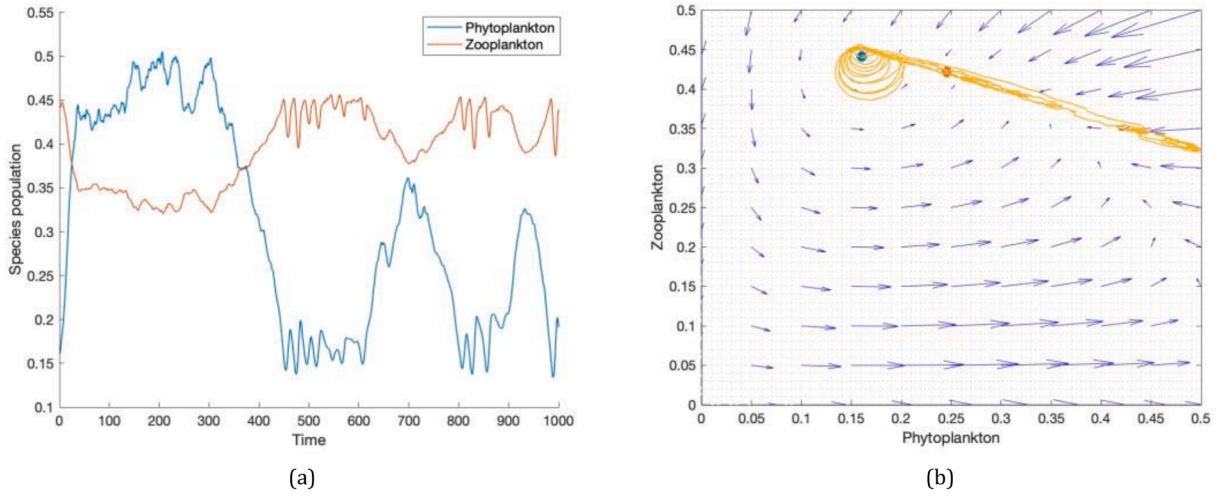


Fig. 10. (a): Population dynamics at Lat 45°. (b): Phase plane at Lat 45°.

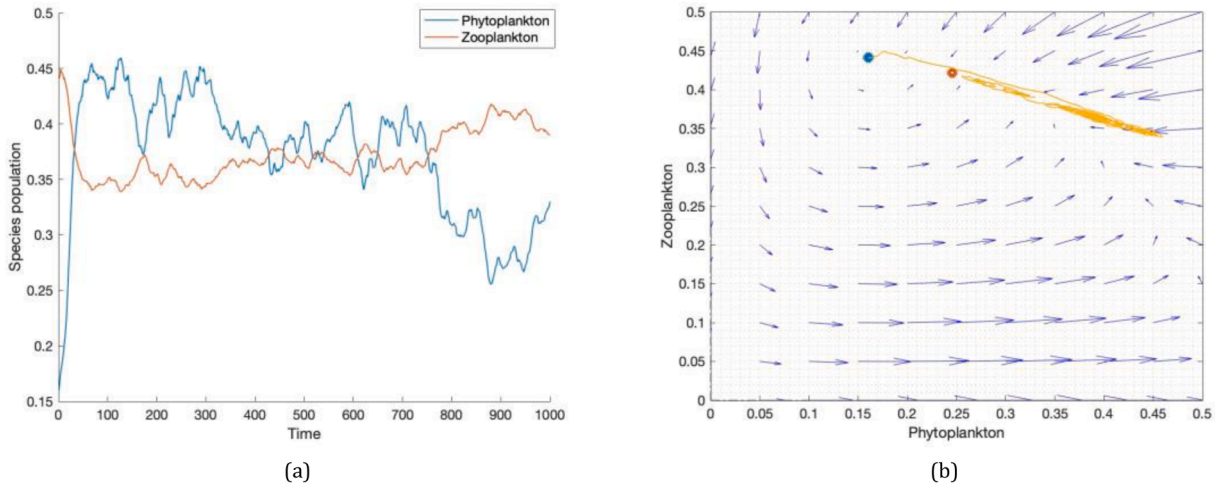


Fig. 11. (a): Population dynamics at Lat 15°. (b): Phase plane at Lat 15°.

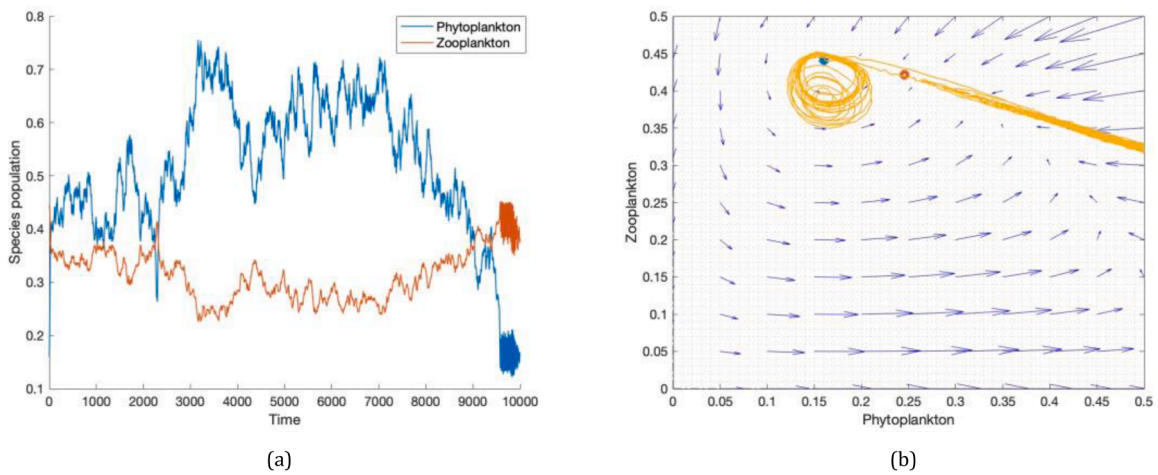


Fig. 12. (a): Population dynamics at Lat 15° - over a much longer time period. (b): Phase plane at Lat 15° over a much longer time period.

random walk around the original K_I value which addresses the fluctuations typical in climate models. As stated in previous Sections, seasonal and daily variations in light are omitted from consideration because $K(t)$

is light-dependent carrying capacity and not directly light intensity. However, the model takes into account noise increasing as latitude increases. When light is incident on the Earth, photons are scattered more

at higher latitudes than at lower latitudes. In other words, the angle of incidence is lower at the equator and at higher latitudes Rayleigh scattering is more prominent.

The noise parameters are defined as

$$\varepsilon_x = 0.001 + \alpha_1, \varepsilon_y = 0.008 + \alpha_2, \varepsilon_K = 0.005(1 + |\sin(\phi)|) \quad (13)$$

where the values for ε_1 and ε_2 are selected as in Section 3.2.

We start with stochastic simulations run for 3 different latitudes where for each latitude 5000 runs were made in conjunction to the mean zonal temperature at each latitude. The results are given in Table 5.

Table 5 shows that one cannot fit a NLM (normal linear model) like in Section 3.1 due to the nonlinear trend of time to first transition. However, an interesting observation arises pertaining to the latitudinal distribution of *phytoplankton*. Table 5 suggests that the optimal place for *phytoplankton* growth is in the mid-latitude region which is supported by Fig. 14. This is because there is sufficient amounts of light throughout the year and moderate temperatures.

It is also important to note that because at latitude 75° , the mean temperature is 10°C , as stated in Table 5. This temperature is outside the optimal temperature range of *phytoplankton* therefore the additional noise parameter must be added to *phytoplankton* for temperature-induced noise as for *zooplankton* (α_2). This is why in Table 5, the mean time to first transition is significantly lower. Notice also that the times to first transition in Table 3 are significantly greater than those of Table 5. This is because of the absence of noise in light-dependent carrying capacity which gives an example of the importance the environment plays on a biological system. With a finer resolution of zonal mean temperature at 1000hPa , Fig. 14 shows evidence supporting the observation surrounding Table 5.

The intrinsic noise for *zooplankton* (ε_2) is significantly larger than that of *phytoplankton* (ε_1).

This is to account for predation on *zooplankton* previously discussed in Section 3.2. The reason why one can assume the existence of a zonal mean temperature is because variation of temperature in water is quite narrow. With this limited variation, one can allow for the parameters defined in Table 1 to remain constant, accounting for limited variation in parameters for the system. By extension, this means that the states E_2 and E_4 are invariant.

5. Discussion

In our work, we have investigated the intrinsic and extrinsic factors that may disbalance the producer-grazer system coupling via environmental changes. To explore how these factors affect these systems in a more real sense we can make use of stochastic models and simulations. For example, the LKE model, whose global dynamics have so far been entirely studied mechanistically by using the Holling type II functional response (Xie et al., 2018), can be extended to take into account the stochastic noise generated by intrinsic/extrinsic factors as a Wiener process. In particular, we explored the different outputs from the stochastic LKE model as a consequence of considering sudden events like predation and wind gusts, as well as macro environmental factors such as the variation of temperature due climate change. We therefore proposed a way in which the LKE model can be extended to account for the change in light-dependent carrying capacity, taking into account the ever-growing prevalence of climate change on life on earth. The

Table 5

Time to first transition range for latitude cells including temperature noise (zonal temperatures adjusted to course zonal resolution of latitude temperatures).

Hadley cell	Latitude	Mean temperature	$\bar{x} \pm \sigma$ (TFT in days)
Hadley/Ferrel cell	15°	30°C	26.4414 ± 4.1589
Mid-Latitude cell	45°	20°C	29.2434 ± 5.2529
Polar cell	75°	10°C	3.7224 ± 1.5402

extension itself is inspired by a simple model of climate change where a saturating function was used.

Intrinsic noise is naturally present in biological systems and we investigated this before adding on extrinsic noise as well. In particular, the time to first transition, which measures how long it takes for the population dynamics to move from the E_2 to E_4 attracting basins, showed that, as the intrinsic noise in *phytoplankton* increased whilst that of *zooplankton* remained constant, can have predictable qualities. More precisely, the time to first transition follows a linear trend to which we fitted a normal linear model. We found that the NLM can be used to predict the time to first transition for small extrapolations. This is a somewhat curious result because whilst TFT inherently relies on the unpredictability of a stochastic system, the behaviour could in fact be made predictable. The simulations corroborated our intuition that the times to first transition should decrease with increasing noise, which meant that we had a certain level of certainty that the model is reasonable and can be extended to consider extrinsic noise.

Similar to intrinsic noise, extrinsic noise is typical in biological systems due to the fact that organisms are inevitably affected by their changing environment. The generalisation of the noise factors on a macro scale was done by basing noise in the system to be attributed to non-biological factors. The reason for this is that when sudden events (predation, weather anomalies) occur, a change in equilibrium would not happen arbitrarily as it depends on the severity of the event. Furthermore, it only influences the system at discrete points in time over the entire time interval considered. For example, this scenario makes the assumption that the fish cohort eats at a constant rate each day (Holling type I assumption) and does not take into account satiation amongst the fish population. It also assumes that the feeding interval of the fish population is uniform, i.e. each fish population that comes across the *zooplankton* population in the model has the same size. Lastly, the model isolates fish as the only source of predation on the *zooplankton* population. Herewith modelling the possible impacts of a changing environment on an ecosystem is a very complicated task at a high resolution. We therefore considered modelling using generalist predators such that we can incorporate a broader scope of predation on *phytoplankton*. This averaging over of the set of predators makes sense since we are investigating the system over a long period of time and predator-prey oscillations are less important compared to net increase/decrease of a species population. On the other hand, temperature and latitudinal-dependent noises influence the system throughout the entire time interval considered ergo are more useful as extrinsic noise generators when applied to mean time to first transition. Simulation-supported evidence for why time to first transition is very important in the context of this paper is shown where despite $K(t)$ increasing from K_L to K_U where K_L, K_U , the system returns to oscillating between the two original steady states E_2 and E_4 .

The major finding of this work is that a simple approximation of extrinsic noise on the system applied to time to first transition yields a curiously adept latitudinal distribution of *phytoplankton* clusters for $Lat \in [(\text{Vadim Anishchenko and Astakhov, 2007}), 50]$ which encompasses most of the major *phytoplankton* clusters in both hemispheres (see Table 6). The results imply that the greater the time to first transition for *phytoplankton* going from low to high abundance at a given latitude, the greater the likelihood of large *phytoplankton* clusters at that latitude ($Lat \in [40]$) and in a small neighbourhood of this latitude range ($\pm 10^\circ$). This is a good generalization of the general trend of *phytoplankton* worldwide, putting forward a way to coalesce noise, time to first transition and resulting latitudinal spatial distribution over a global scale. The novelty of this approach may have implications for how noise can be used as a tool for understanding the behaviour of biological systems in relation to the environment. To produce our results, we are considering the impact of temperature, latitude and the influence of light on our biological system. These three factors are inter-related where light intensity and temperature generally decrease away from the equator. For simplicity we considered how the system would be affected under different

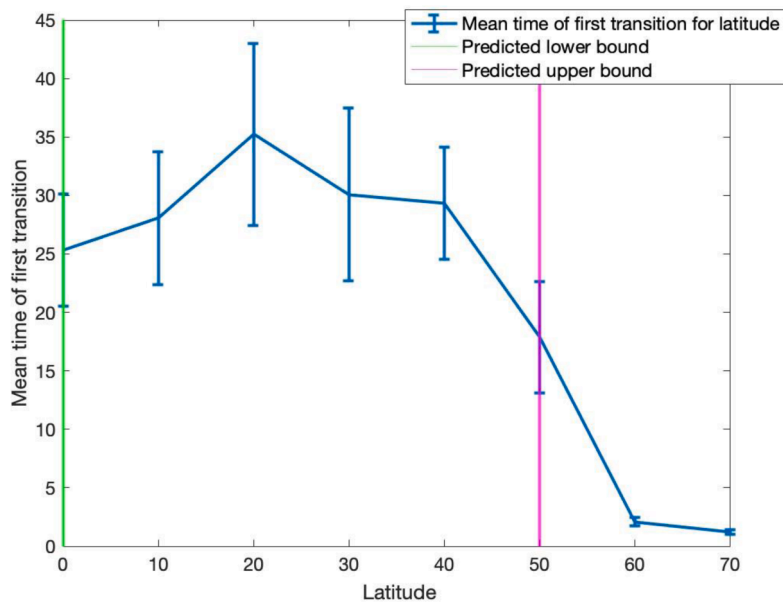


Fig. 13. Latitude-dependent time to first transition; temperature only for full LKE model.

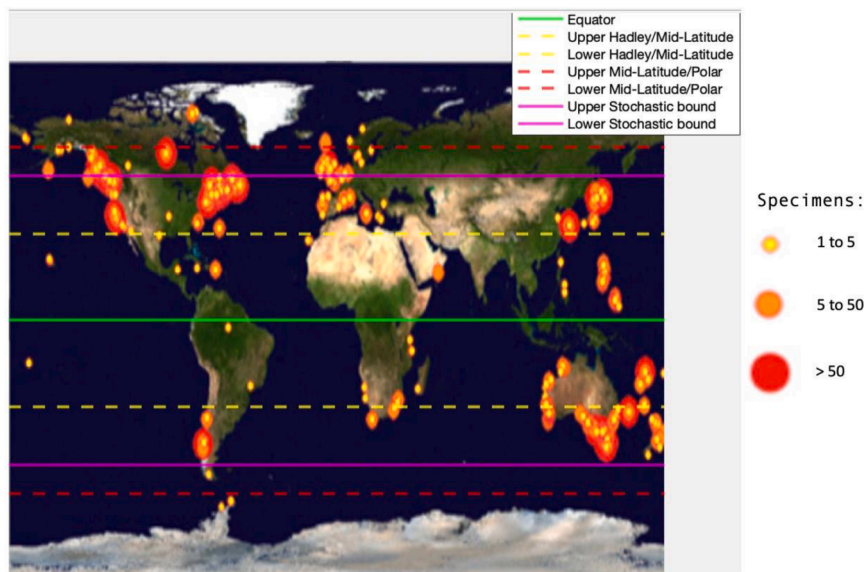


Fig. 14. Summary graph adapted from <http://www2.unb.ca/cemar/saunders/alga.html>.

Table 3

Numerical values of the parameters with definitions - data is plotted in Fig. 5 applied to Eq. (6) with $\dot{K} = 0$.

X	y	$\bar{x} \pm \sigma$ (Time to first transition (TFT) in days)
0.001	0.008	828.7086 ± 62.6393
0.002	0.008	808.0934 ± 54.8289
0.003	0.008	801.1098 ± 53.6047
0.004	0.008	779.1328 ± 67.3376
0.005	0.008	783.4590 ± 62.2270
0.006	0.008	731.2970 ± 59.6108
0.007	0.008	717.0018 ± 61.7820
0.008	0.008	688.0580 ± 56.7747

scenarios where temperature and light-dependent carrying capacity are parameterised by latitude. Temperature was considered slightly differently in the final results such that data from literature can be used.

Table 6

Time to first transition range for latitude cells including temperature noise with a finer resolution of zonal mean temperature at 1000hPa (zonal mean temperature from Pielke re-search group, <https://pielkeclimatesci.wordpress.com/2012/07/11/sea-surface-temperature-trends-as-a-function-oflatitude-bands-by-roger-a-pielke-sr-and-bob-tisdale/>) for the full LKE model.

Latitude	Mean temperature	$\bar{x} \pm \sigma$ (TFT in days)
00	28°C	25.3092 ± 4.7819
10°	28°C	28.0650 ± 5.6947
20°	26°C	35.2322 ± 7.7812
30°	23°C	30.0870 ± 7.3732
40°	20°C	29.3326 ± 4.7954
50°	15°C	17.8696 ± 4.7736
60°	10°C	2.0884 ± 0.3554
70°	2°C	1.1920 ± 0.2008

Apart from the general trend of *phytoplankton* clusters, the use of extrinsic noise in the context of time to first transition also indicates the presence of arctic amplification wherein the northern hemisphere is warming up at a greater rate than anywhere else on earth. In order to help with analysis of the latitudinal distribution of *phytoplankton*, we took into account the earth's weather system which is divided into Hadley cells: Ferrel (or Hadley) cells, Mid-Latitude cells, and Polar cells. Each cell spans 30° latitude in each of the Earth's hemispheres (the boundaries of these cells are illustrated in Fig. 14). Polar cells are the weakest (most likely to change of all the types of Hadley cells) and in the presence of climate change, a possible long-term impact is that the (northern) polar cell's lower latitude of 60° may increase hence leading to larger *phytoplankton* clusters found at higher latitudes due to arctic amplification which is the second major result of the paper. This is evident when the stochastic bounds as a result of TFT are superimposed on the global *phytoplankton* audit. Fig. 14 has some evidence that there is clear *phytoplankton* clusters over-spill above 50° in the northern hemisphere whilst in the southern hemisphere, the large *phytoplankton* clusters are bounded by 50° . This asymmetry in latitudinal distribution is indicative of the influence of 'arctic amplification' on the latitudinal distribution of *phytoplankton*. It is clear that the northern hemisphere *phytoplankton* distribution is better suited to Hadley cell stratification in the upper bound.

An improvement to the model would take into account other source forms of extrinsic noise such as moisture as well as climatological models. Factoring in favourable environmental conditions for the meridional distribution would require extending the spatially homogeneous model to a spatially heterogeneous model as well as the additional collection of meteorological data. The consideration of other extrinsic noise would provide a more comprehensive model of the environment, leading to more accurate results such as considering nutrient density zonally as well. Both empirical and theoretical studies in this direction are appealing.

CRedit authorship contribution statement

Velizar Kirkow: Conceptualization, Methodology, Writing – original draft, Writing – review & editing. **Hao Wang:** Supervision, Investigation, Writing – review & editing. **Pablo Venegas Garcia:** Supervision, Investigation, Writing – review & editing. **Shohel Ahmed:** Supervision, Investigation, Writing – review & editing. **Christopher M. Heggerud:** Supervision, Investigation, Writing – review & editing.

Declaration of Competing Interest

The authors declare that they have no known competing financial interests or personal relationships that could have appeared to influence the work reported in this paper.

Bibliography

- Bellouin, N., Quaas, J., Gryspeerdt, E., Kinne, S., Stier, P., Watson-Parris, D., Boucher, O., Carslaw, K.S., Christensen, M., Daniau, A.-L., et al., 2020. Bounding global aerosol radiative forcing of climate change. *Reviews of Geophysics* 58 (1) e2019RG000660.
- Blottiere, L., 2015. The effects of wind-induced mixing on the structure and functioning of shallow freshwater lakes in a context of global change. Ph.D. thesis. Université Paris-Saclay.
- Chapman, E.J., Byron, C.J., 2018. The flexible application of carrying capacity in ecology. *Global Ecology and Conservation* 13, e00365.
- Costa, L., Huszar, V., Ovalle, A., 2009. Phytoplankton functional groups in a tropical estuary: hydrological control and nutrient limitation. *Estuaries and Coasts* 32 (3), 508–521.
- Dawes, J., Souza, M., 2013. A derivation of Holling's type I, II and III functional responses in predator-prey systems. *Journal of Theoretical Biology* 327, 11–22.
- Edelstein-Keshet, L., 2005. *Mathematical Models in Biology*. Society for Industrial and Applied Mathematics.

- Elser, J., Kuang, Y., 2002. Ecological stoichiometry. *Encyclopedia of Theoretical Ecology* 84, 718–722.
- Gao, J.B., Hwang, S.K., Liu, J.M., 1999. When can noise induce chaos? *Phys. Rev. Lett.* 82, 1132–1135.
- Gottwald, G.A., Harlim, J., 2013. The role of additive and multiplicative noise in filtering complex dynamical systems. *Proceedings of the Royal Society A: Mathematical, Physical and Engineering Sciences* 469 (2155), 20130096.
- Hartmann, S., Beasley, A., Mozhayeva, D., Engelhard, C., Witte, K., 2020. Defective defence in *Daphnia* daughters: silver nanoparticles inhibit anti-predator defence in offspring but not in maternal *Daphnia magna*. *Scientific Reports* 10 (1), 1–9.
- Horsthemke, W., 1984. *Noise-Induced Transitions*. Springer-Verlag Berlin Heidelberg.
- Khan, Q., Khan, M., 2008. Effect of temperature on waterflea *Daphnia magna* (Crustacea: Cladocera). *Nature Precedings* 1–1–1.
- Kim, S., Park, S.H., Ryu, C.S., 1998. Colored-noise-induced multistability in nonequilibrium phase transitions. *Phys. Rev. E* 58, 7994–7997.
- Kraut, S., Feudel, U., 2002. Multistability, noise, and attractor hopping: The crucial role of chaotic saddles. *Phys. Rev. E* 66, 015207.
- Lecar, H., 2007. Morris-lecar model. *Scholarpedia* 2 (10), 1333.
- Lei, X., Tian, W., Zhu, H., Chen, T., Ao, P., 2015. Biological sources of intrinsic and extrinsic noise in ci expression of lysogenic phage lambda. *Scientific Reports* 5 (1), 1–12.
- Li, X., Wang, H., Kuang, Y., 2011. Global analysis of a stoichiometric producer-grazer model with Holling type functional responses. *Journal of Mathematical Biology* 63 (5), 901–932.
- Loladze, I., Kuang, Y., Elser, J.J., 2000. Stoichiometry in producer-grazer systems: linking energy flow with element cycling. *Bulletin of Mathematical Biology* 62 (6), 1137–1162.
- Marshall, J., Plumb, R.A., 1989. *Atmosphere, ocean and climate dynamics: an introductory text*. Academic Press.
- Metsoviti, M.N., Papapolymerou, G., Karapanagiotidis, I.T., Katsoulas, N., 2020. Effect of light intensity and quality on growth rate and composition of *Chlorella vulgaris*. *Plants* 9 (1), 31.
- T. Palmer, P. D. Williams, *Introduction. stochastic physics and climate modelling* (2008).
- Sabino, A.U., Vasconcelos, M.F., Sittoni, M.Y., Lautenschlager, W.W., Queiroga, A.S., Morais, M.C., Ramos, A.F., 2018. Lessons and perspectives for applications of stochastic models in biological and cancer research. *Clinics* 73.
- Singh, S., Singh, P., 2015. Effect of temperature and light on the growth of *algae* species: a review. *Renewable and Sustainable Energy Reviews* 50, 431–444.
- Sterner, R.W., Elser, J.J., 2017. *Ecological stoichiometry*. Princeton university press.
- Urabe, J., Elser, J., Kyle, M., Yoshida, T., Sekino, T., Kawabata, Z., 2002. Herbivorous animals can mitigate unfavourable ratios of energy and material supplies by enhancing nutrient recycling. *Ecology Letters* 5, 177–185.
- Vadim Anishchenko, A.N.T.V.L.S.-G., Astakhov, Vladimir, 2007. *Nonlinear Dynamics of Chaotic and Stochastic Systems*. Springer, Berlin.
- Wang, H., Liu, M., 2020. Stationary distribution of a stochastic hybrid phytoplankton-zooplankton model with toxin-producing phytoplankton. *Applied Mathematics Letters* 101, 106077.
- Wei, P.-S., Hsieh, Y.-C., Chiu, H.-H., Yen, D.-L., Lee, C., Tsai, Y.-C., Ting, T.-C., 2018. Absorption coefficient of carbon dioxide across atmospheric troposphere layer. *Heliyon* 4 (10), e00785.
- Xie, T., Yang, X., Li, X., Wang, H., 2018. Complete global and bifurcation analysis of a stoichiometric predator-prey model. *Journal of Dynamics and Differential Equations* 30 (2), 447–472.
- Xingwang Yu, S.Y., 2020. Asymptotic properties of a stochastic chemostat model with two distributed delays and nonlinear perturbation. *Discrete Continuous Dynamical Systems - B* 25 (7), 2373–2390.
- Xingwang Yu, T.Z., Yuan, Sanling, 2018. The effects of toxin-producing phytoplankton and environmental fluctuations on the planktonic blooms. *Nonlinear Dynamics* 91, 1653–1668.
- Xu, C., Yuan, S., 2016. Competition in the chemostat: A stochastic multi-species model and its asymptotic behavior. *Mathematical Biosciences* 280, 1–9.
- Xu, C., Yuan, S., Zhang, T., 2016. Stochastic sensitivity analysis for a competitive turbidostat model with inhibitory nutrients. *International Journal of Bifurcation and Chaos* 26 (10), 1650173.
- Yu Zhao, J.M., Yuan, Sanling, 2015. Survival and stationary distribution analysis of a stochastic competitive model of three species in a polluted environment. *Bulletin of Mathematical Biology* 77, 1285–1326.
- Yu, X., Yuan, S., Zhang, T., 2019. Survival and ergodicity of a stochastic phytoplankton-zooplankton model with toxin-producing phytoplankton in an impulsive polluted environment. *Applied Mathematics and Computation* 347, 249–264.
- Yu, X., Yuan, S., Zhang, T., 2019. Asymptotic properties of stochastic nutrient-plankton food chain models with nutrient recycling. *Nonlinear Analysis: Hybrid Systems* 34, 209–225.
- Yuan, S., Wu, D., Lan, G., Wang, H., 2020. Noise-induced transitions in a nonsmooth producer-grazer model with stoichiometric constraints. *Bulletin of Mathematical Biology* 82 (5), 1–22.
- Zhao, D., Liu, H., 2019. Coexistence in a two species chemostat model with markov switchings. *Applied Mathematics Letters* 94, 266–271.